ACS APPLIED MATERIALS & INTERFACES

Letter

www.acsami.org

Solvent-Free Click-Mechanochemistry for the Preparation of Cancer Cell Targeting Graphene Oxide

Noelia Rubio,[†,‡] Kuo-Ching Mei,[†,‡] Rebecca Klippstein,[‡] Pedro M. Costa,[‡] Naomi Hodgins,[‡] Julie Tzu-Wen Wang,[‡] Frederic Festy,[§] Vincenzo Abbate,[‡] Robert C. Hider,[‡] Ka Lung Andrew Chan,[‡] and Khuloud T. Al-Jamal*[,‡]

[‡]Institute of Pharmaceutical Science, King's College London, Franklin-Wilkins Building, 150 Stamford Street, London SE1 9NH, United Kingdom

[§]Biomaterials, Biomimetics and Biophotonics Division, Dental Institute, King's College London, London SE1 9RT, United Kingdom

Supporting Information

ABSTRACT: Polyethylene glycol-functionalized nanographene oxide (PEGylated n-GO) was synthesized from alkyne-modified n-GO, using solvent-free click-mechanochemistry, i.e., copper(I)-catalyzed azide−alkyne cycloaddition (CuAAC). The modified n-GO was subsequently conjugated to a mucin 1 receptor immunoglobulin G antibody (anti-MUC1 IgG) via thiol−ene coupling reaction. n-GO derivatives were characterized with Fourier-transformed infrared (FT-IR) spectroscopy, thermogravimetric analysis (TGA), Bradford assay, sodium dodecyl sulfate polyacrylamide gel electrophoresis (SDS-PAGE), and atomic force microscopy (AFM). Cell targeting was confirmed in vitro in MDA-MB-231 cells, either expressing or lacking MUC1 receptors, using flow cytometry, confocal laser scanning microscopy (CLSM) and multiphoton (MP) fluorescence microscopy. Biocompatibility was assessed using the modified lactate dehydrongenase (mLDH) assay.

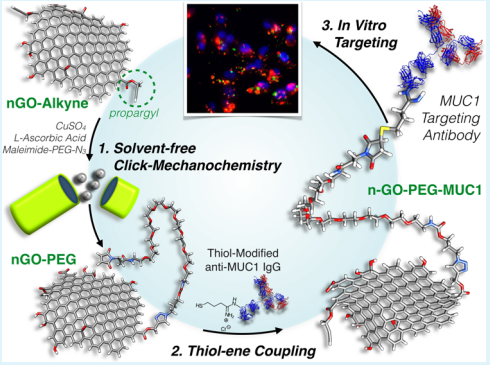

KEYWORDS: *antibody, nanomedicine, drug delivery, toxicity, breast cancer*

Graphene is a novel two-dimensional (2D) nanomaterial formed from a single layer of carbon atoms. It has attracted the attention of scientists working in different fields since the first observation of graphene by Boehm-Hofmann[1] and the discovery of single layer isolation.[2] Graphene oxide (GO) is useful in biomedical applications because of its good dispersibility in aqueous media and easy modification of its functional groups.[3] GO constitutes a promising material in fields such as photothermal anticancer therapy,[4] drug delivery,[5] and gene delivery.[6] Selectivity in cancer cell targeting remains an unmet need thus preparation of nanocarriers capable of efficient and selective targeting of cancer cells is highly desirable.[7] Achieving this aim using facile and eco-friendly (solvent-free) chemical methods adds value to the whole approach.

In this work, PEGylated GO was successfully synthesized, for the first time, using the solvent-free click-mechanochemistry approach. Azide- and maleimide-terminated bifunctional PEG polymer was synthesized and characterized using ^{1}H NMR and FT-IR spectroscopy (Figure S1). GO was synthesized using a modified Kovtyukhova-Hummer's method that we have reported previously.[8] The carboxylic groups available in GO were coupled to propargyl alcohol using the Steglich esterification reaction,[9] yielding n-GO-alkyne (Scheme 1).

FT-IR spectroscopy was used to confirm that the alkyne group was introduced on the GO. However, the alkyne signal at 3292 cm^{-1} was masked by the O−H band from GO. For this reason deuterium conversion was used to assess the presence of alkyne groups introduced on GO (Figure 1A) as the new C−D band displays a stronger signal at 2565 cm^{-1} compared with the

Scheme 1. Synthesis of the PEGylated Nano-graphene Oxide Targeting MUC1 (n-GO-PEG-MUC1)

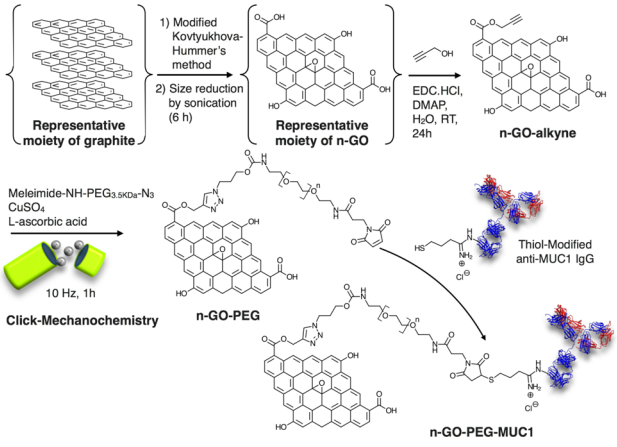

Received: July 11, 2015
Accepted: August 17, 2015
Published: August 17, 2015

DOI: 10.1021/acsami.5b06250
ACS Appl. Mater. Interfaces 2015, 7, 18920−18923

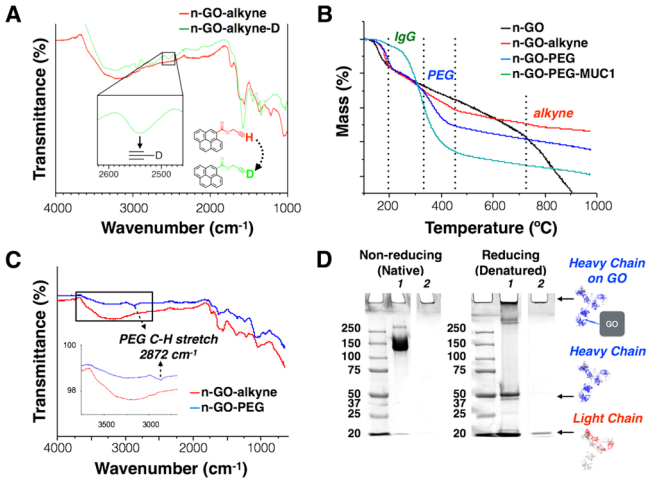

Figure 1. Characterization of n-GO derivatives. (A) FT-IR measurements of n-GO-alkyne before and after deuteration; (B) TGA graphs; (C) FT-IR measurements of n-GO-alkyne before and after click reaction. (D) SDS-PAGE gel electrophoresis under nonreducing (right) and reducing (left) conditions of anti-MUC1 IgG (1) and n-GO-PEG-MUC1 (2).

initial C−H band. The terminal hydrogen was replaced by deuterium following a mild and efficient protocol described by Bew et al.[10] (Figure S2A). The FT-IR spectrum (Figure S2A, top panel) showed the appearance of a peak at 2565 cm^{-1} due to the vibration of the C−D bond, proving the conversion of propargyl alcohol to ^{2}H-propargyl alcohol. Figure S2A shows the GO-alkyne spectrum with a new band appearing at 2565 cm^{-1}, after deuteration that corresponds to the vibration of the bond C−D. The O−H of GO may also be converted to O−D, which overlaps with the C−D bond. To eliminate this possibility, we subjected GO (lacking alkyne) to deuteration reaction conditions. No band was detected at 2565 cm^{-1} (Figure S2B), suggesting that the previously observed peak at 2565 cm^{-1} was due to the deuterium conversion.

Thermogravimetric analysis (TGA) (Figure 1B) showed typical TGA profile of GO, which agreed with previously published data. An initial decrease at 200 °C was associated with the removal of carboxylic/alcohol/epoxy groups.[11] A second decrease at 700 °C was due to the decomposition of the graphitic skeleton of GO. Esterification reaction with propargyl alcohol yielding n-GO-alkyne resulted in an increase in the thermal stability at the highest temperatures.

Subsequently, the maleimide/azide heterofunctionalized polyethylene glycol (maleimide-NH-$PEG_{3.5KDa}$-N_3) was introduced on n-GO-alkyne using solvent-free click-mechanochemistry namely the copper(I)-catalyzed azide−alkyne cycloaddition (CuAAC). Click-mechanochemistry has been applied widely on small organic molecules[12] but has never been employed to modify GO. The resulting n-GO-PEG showed an increase in weight loss from 46 to 55%, at 600 °C, confirming PEG introduction to GO (which corresponds to a PEG content of 31 μmol per gram n-GO). The presence of PEG was confirmed by FT-IR spectroscopy (Figure 1C); the peak of C−H stretching vibration was clearly observed at 2872 cm^{-1}. Functionalization of n-GO-alkyne with PEG polymer enhanced the aqueous dispersibility of the system. The final concentration of the prepared n-GO-alkyne and n-GO-PEG was 0.3 and 0.75 mg/mL, respectively.

Anti-MUC1 IgG antibody was conjugated to the maleimide addends using a thiol−ene coupling reaction, yielding n-GO-PEG-MUC1. An increase in the weight loss from 55 to 71%, was observed due to the antibody introduction to n-GO, corresponding to 160.5 μg antibody per gram n-GO. Anti-MUC1 IgG loading was also quantified using Bradford protein assay (Figure S4). This assay is based on the change of the absorbance of the Coomassie Blue dye when binding to proteins.[13] The increase in the absorption peak observed at 545 nm corresponded to 165.2 μg antibody per gram n-GO, which correlates well with the amount calculated from TGA. Covalent conjugation to anti-MUC1 IgG further enhanced the aqueous dispersibility so that the final concentration achieved for n-GO-PEG-MUC1 was 1.05 mg/mL.

The structural properties of the n-GO conjugates were studied using Raman spectroscopy (Figure S3A). Typical D (1317 cm^{-1}) and G (1610 cm^{-1}) bands were observed, corroborating that the graphitic structure of the layers was preserved after mechanochemistry and subsequent IgG functionalization. I_D/I_G peak height ratio for n-GO was 1.52 ± 0.06 (n = 3, n corresponds to the number of Raman spectra recorded), which is similar to n-GO-alkyne (I_D/I_G ratio = 1.59 ± 0.03, n = 3) and n-GO-PEG (I_D/I_G ratio = 1.52 ± 0.04, n = 3) derivatives. This fact suggests that the structural properties of the n-GO are maintained after the milling process, which agrees with our preliminary n-GO-mechanochemistry studies.[8] AFM measurements using the tapping mode (in air) were performed in order to study the morphological properties. A maximum/medium size of 2.15 μm^2/62 nm^2 was found for n-GO, after 4 h bath sonication (n = 621).[14] The height images of n-GO-PEG and n-GO-PEG-MUC1 are shown in Figure S3B.

SDS-PAGE electrophoresis under denaturing/reducing (protein separation based on mass differences) and native/nonreducing (protein separation based on mass-charge ratio) conditions was performed to analyze the interactions between GO and the anti-MUC1 IgG antibody (Figure 1D). No bands were observed for n-GO-PEG-MUC1 under nonreducing conditions. The typical heavy and light chains were, as expected, observed when carrying out the electrophoresis under denaturing/reducing conditions. The results confirmed the stable conjugation of the antibody and n-GO-PEG. To further confirm the covalent conjugation between n-GO-PEG-maleimide and the thiolated antibody (through thiol-maleimide coupling), a mixing control study was performed using n-GO-PEG-NH_2 (lacking the maleimide group) and the thiolated anti-MUC1 IgG. The result was analyzed using SDS-PAGE under reducing condition (Figure S5). Signals for both the heavy and light chains were seen only in the mixing control (Figure S5, lane 2). In the conjugate n-GO-PEG-MUC1 (Figure S5, lane 3), only a faint signal for the light chain can be seen, as the heavy chains were immobilized on the PEG covalently.

The toxicity of the GO samples on breast cancer cell lines MDA-MB-231-ME (MUC1+) and MDA-MB-231 (MUC1−) was evaluated using the modified LDH assay (Figure S6). Dimethyl sulfoxide (DMSO) (10% v/v) was used as a positive toxic control. No significant toxicity (<15% cell death) was observed on cells incubated with n-GO-PEG and n-GO-PEG-MUC1 at 10 μg/mL for 24 or 72 h, whereas higher concentrations, i.e., 50 and 100 μg/mL, showed significant dose- and time-dependent toxicity (Figure S6). MUC1+ cells were found to be more sensitive to targeted and nontargeted n-GO than MUC1− cells. Moreover, n-GO-PEG-MUC1

DOI: 10.1021/acsami.5b06250
ACS Appl. Mater. Interfaces 2015, 7, 18920−18923

exhibited a higher toxicity with MUC1+ cells (for the three tested concentrations) when compared that with n-GO-PEG. This effect was more pronounced and statistically significant at 72 h ($p < 0.01$ for 10 μg/mL, $p < 0.001$ for 50 and 100 μg/mL).

The n-GO-PEG-MUC1 sample was further tested in the two MDA-MB-231 breast cancer cell lines in order to confirm the intracellular delivery and the possible targeting effect. Cells were imaged using confocal laser scanning microscopy (CLSM) and MP fluorescence microscopy in order to detect the anti-MUC1 IgG antibody and GO, respectively (Figure 2). The

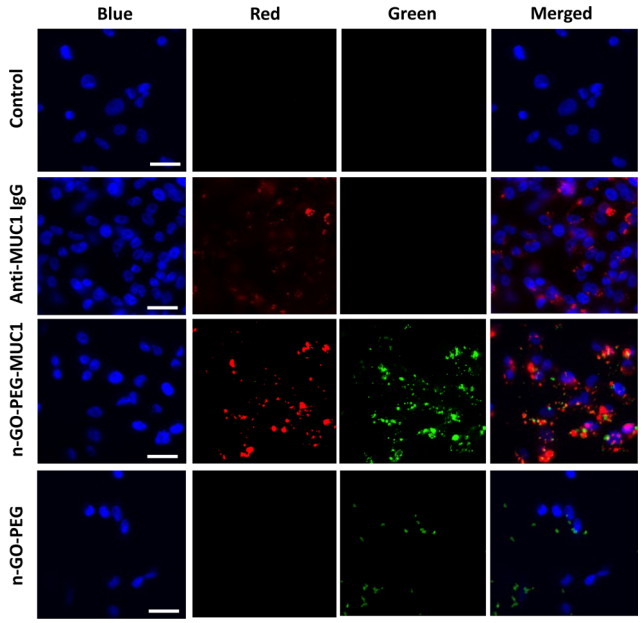

Figure 2. Confocal laser scanning microscopy (CLSM) and multiphoton (MP) fluorescence microscopic images of MUC1+ cells incubated with anti-MUC1 IgG, n-GO-PEG or n-GO-PEG-MUC1. MUC1+ cells were incubated with individual treatments for 3 h then stained with Cy3 labeled antihuman IgG (H+L) (red) and DAPI (nuclei, blue) and imaged with CLSM (anti-MUC1 IgG, red) or MP microscopy (GO, green). Objective used was 40×/1.25 NA. Scale bars = 15 μm.

multiphoton emission properties of GO have been recently described;[15] these studies demonstrated the broad emission spectra of GO in the visible range, when excited using a femtosecond laser. We have relied on these optical properties for the detection of GO in cells. MUC1+ cells were incubated with anti-MUC1 IgG, n-GO-PEG or n-GO-PEG-MUC1, at concentrations equivalent to 2.5 μg/mL anti-MUC1 IgG for 3 h. This was equivalent to 10 μg/mL n-GOs, a concentration that has proven to be nontoxic to cells under these conditions. Cells were then fixed, permeabilized and immunostained with cyanine dye (Cy3)-labeled antihuman IgG, to track anti-MUC1 antibody. 4′-6-Diamidino-2-phenylindole (DAPI) was used to visualize the nucleus (CLSM). Direct imaging of GO was carried out using MP (green channel). The free antibody was internalized in cells within 3 h of incubation. Stronger green signals were detected in cells incubated with n-GO-PEG-MUC1 than n-GO-PEG (Figure 2), suggesting higher specificity of the former. CLSM confirmed the presence of anti-MUC1 IgG within the cells (red channel), red signals corresponding with anti-MUC1 IgG colocalized with the green signals of n-GO-PEG-MUC1, corroborating that anti-MUC1 IgG remained conjugated to n-GO-PEG after cellular internalization. As expected, no red signals were observed for n-GO-PEG (lacking the antibody). Images showing uptake in MUC1− cells are shown in Figure S7. No uptake of anti-MUC1 IgG (red channel) was observed in this instance because of the absence of MUC1 receptors. The same cells showed reduced uptake of n-GO-PEG-MUC1 than in MUC1+ cells adding further confirmation of the targeting effect of n-GO-PEG-MUC1.

The uptake of n-GO-PEG-MUC1 in MUC1+ cells was also assessed by flow cytometry and the extent of uptake was expressed as mean fluorescence intensity (MFI) (Figure 3).

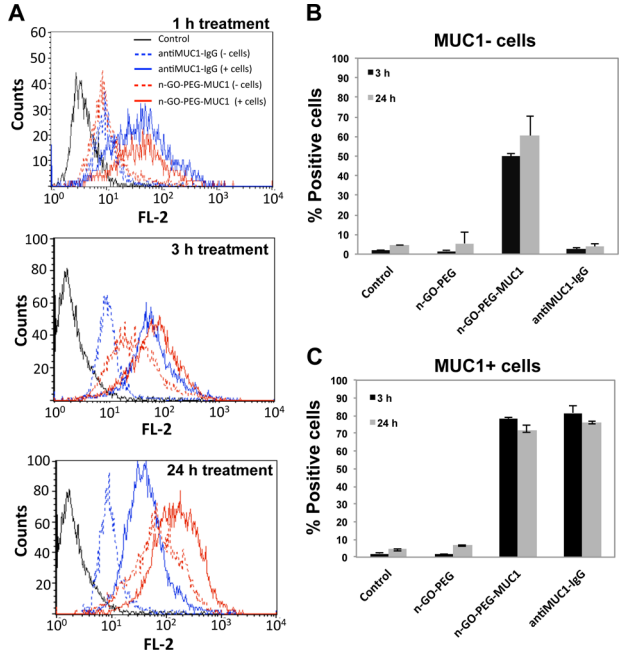

Figure 3. Intracellular uptake of n-GO-PEG-MUC1 in MUC1+ and MUC1- human breast cancer cells in vitro. (A) Flow cytometric profiles of MUC1+ and MUC1- cell lines treated with antiMUC1-IgG or GO-PEG-MUC1 for 1 h, 3 or 24 h. Cellular uptake was assessed by analyzing the shift in mean fluorescence intensity (MFI). The percentage of positive cells for MUC1− and MUC1+ cells are shown in (B) and (C). Signals were collected using FL2 detector.

Cells were treated for 1, 3, and 24 h with anti-MUC1 IgG or n-GO-PEG-MUC1 at concentrations equivalent to 2.5 μg/mL anti-MUC1 IgG. n-GO-PEG was used as a control. At 1 h, comparable results were obtained for both anti-MUC1 IgG and n-GO-PEG-MUC1 with uptake only being observed in MUC1+ cells. At 3 h, an increase in MFI was found in MUC1− cells treated with n-GO-PEG-MUC1. This increase in MFI, however, was significantly lower than that observed in MUC1+ cells. At 24 h, MUC1+ cells treated with n-GO-PEG-MUC1 showed significantly higher MFI values compared to all treatment groups (Figure 3A), agreeing with CLSM and MP results.

In summary, PEGylation of GO using click-mechanochemistry in the absence of solvents is demonstrated successfully for the first time. Targeting breast cancer cells in vitro is accomplished through the introduction of an anti-MUC1 IgG. Selectivity to MUC1+ cells, at nontoxic concentrations, was confirmed using a variety of techniques including flow cytometry, CLSM, and MP imaging. The attractive chemical

DOI: 10.1021/acsami.5b06250
ACS Appl. Mater. Interfaces 2015, 7, 18920−18923

approach used for functionalizing nGO combined with the ability to selectively targeticancer cells in vitro are prerequisite for further in vivo evaluation.

■ ASSOCIATED CONTENT

Supporting Information

The Supporting Information is available free of charge on the ACS Publications website at DOI: 10.1021/acsami.5b06250.

Materials used for the development of this work, synthetic routes to produce functionalized n-GO, techniques used to characterize the n-GO conjugates, and supplementary figures (PDF)

■ AUTHOR INFORMATION

Corresponding Author

*E-mail: khuloud.al-jamal@kcl.ac.uk.

Author Contributions

†N.R. and K.-C.M. contributed equally

Notes

The authors declare no competing financial interest.

■ ACKNOWLEDGMENTS

K.T.A.J. acknowledges funding from Biotechnology and Biological Sciences Research Council (BB/J008656/1), Worldwide Cancer Research (12-1054) and the EU FP7-ITN Marie-Curie Network programme RADDEL (290023). K.-C.M. and N.H. are holders of the Graduate School International Research Award (GSIRA) and King's Health Partner's studentship, respectively. P.M.C. is a Sir Henry Wellcome Postdoctoral fellow (WT103913). F.F. acknowledges funding from European Metrology Research Program (NEW02-REG3), Engineering and Physical Sciences Research Council (EP/I014470/1) and Wellcome Trust Medical Engineering Centre.

■ REFERENCES

(1) Boehm, H. P.; Clauss, A.; Fischer, G. O.; Hofmann, U. Das Adsorptionsverhalten sehr dünner Kohlenstoff-Folien. *Z. Anorg. Allg. Chem.* **1962**, *316*, 119−127.

(2) Novoselov, K. S.; Geim, A. K.; Morozov, S. V.; Jiang, D.; Zhang, Y.; Dubonos, S. V.; Grigorieva, I. V.; Firsov, A. A. Electric Field Effect in Atomically Thin Carbon Films. *Science* **2004**, *306*, 666−669.

(3) Dreyer, D. R.; Park, S.; Bielawski, C. W.; Ruoff, R. S. The Chemistry of Graphene Oxide. *Chem. Soc. Rev.* **2010**, *39*, 228−240.

(4) Qin, X. C.; Guo, Z. Y.; Liu, Z. M.; Zhang, W.; Wan, M. M.; Yang, B. W. Folic Acid-Conjugated Graphene Oxide for Cancer Targeted Chemo-Photothermal Therapy. *J. Photochem. Photobiol., B* **2013**, *120*, 156−162.

(5) Yang, X. Y.; Zhang, X. Y.; Ma, Y. F.; Huang, Y.; Wang, Y. S.; Chen, Y. S. Superparamagnetic Graphene Oxide-Fe3O4 Nanoparticles Hybrid for Controlled Targeted Drug Carriers. *J. Mater. Chem.* **2009**, *19*, 2710−2714.

(6) Xu, Y. X.; Wu, Q. O.; Sun, Y. Q.; Bai, H.; Shi, G. Q. Three-Dimensional Self-Assembly of Graphene Oxide and DNA into Multifunctional Hydrogels. *ACS Nano* **2010**, *4*, 7358−7362.

(7) Fay, F.; Scott, C. J. Antibody-Targeted Nanoparticles for Cancer Therapy. *Immunotherapy* **2011**, *3*, 381−394.

(8) Mei, K.-C.; Guo, Y.; Bai, J.; Costa, P. M.; Kafa, H.; Protti, A.; Hider, R. C.; Al-Jamal, K. T. Organic Solvent-Free, One-Step Engineering of Graphene-Based Magnetic-Responsive Hybrids Using Design of Experiment-Driven Mechanochemistry. *ACS Appl. Mater. Interfaces* **2015**, *7*, 14176−14181.

(9) Neises, B.; Steglich, W. Simple Method for the Esterification of Carboxylic Acids. *Angew. Chem., Int. Ed. Engl.* **1978**, *17*, 522−524.

(10) Bew, S. P.; Hiatt-Gipson, G. D.; Lovell, J. A.; Poullain, C. Mild Reaction Conditions for the Terminal Deuteration of Alkynes. *Org. Lett.* **2012**, *14*, 456−459.

(11) Wojtoniszak, M.; Chen, X. C.; Kalenczuk, R. J.; Wajda, A.; Lapczuk, J.; Kurzewski, M.; Drozdzik, M.; Chu, P. K.; Borowiak-Palen, E. Synthesis, Dispersion, and Cytocompatibility of Graphene Oxide and Reduced Graphene Oxide. *Colloids Surf., B* **2012**, *89*, 79−85.

(12) Thorwirth, R.; Stolle, A.; Ondruschka, B.; Wild, A.; Schubert, U. S. Fast, Ligand- and Solvent-Free Copper-Catalyzed Click Reactions in a Ball Mill. *Chem. Commun.* **2011**, *47*, 4370−4372.

(13) Bradford, M. M. Rapid and Sensitive Method for Quantitation of Microgram Quantities of Protein Utilizing Principle of Protein-Dye Binding. *Anal. Biochem.* **1976**, *72*, 248−254.

(14) Mei, K.-C.; Rubio, N.; Costa, P. M.; Kafa, H.; Abbate, V.; Festy, F.; Bansal, S.; Hider, R.; Al-Jamal, K. T. Synthesis of Double-Clickable Functionalised Graphene Oxide for Biological Applications. *Chem. Commun.* **2015**, DOI: 10.1039/C5CC05412E.

(15) Qian, J.; Wang, D.; Cai, F. H.; Xi, W.; Peng, L.; Zhu, Z. F.; He, H.; Hu, M. L.; He, S. L. Observation of Multiphoton-Induced Fluorescence from Graphene Oxide Nanoparticles and Applications in In Vivo Functional Bioimaging. *Angew. Chem., Int. Ed.* **2012**, *51*, 10570−10575.

DOI: 10.1021/acsami.5b06250
ACS Appl. Mater. Interfaces 2015, 7, 18920−18923